Published OnlineFirst July 3, 2012; DOI: 10.1158/1078-0432.CCR-12-0084

Cancer Therapy: Clinical

Clinical Cancer Research

A Tumor Growth Inhibition Model for Low-Grade Glioma Treated with Chemotherapy or Radiotherapy

Benjamin Ribba[1], Gentian Kaloshi[6], Mathieu Peyre[2], Damien Ricard[7], Vincent Calvez[1], Michel Tod[3,4], Branka Čajavec-Bernard[1], Ahmed Idbaih[6], Dimitri Psimaras[6], Linda Dainese[8], Johan Pallud[9], Stéphanie Cartalat-Carel[2], Jean-Yves Delattre[6], Jérôme Honnorat[2,4,5], Emmanuel Grenier[1], and François Ducray[2,4,5]

Abstract

Purpose: To develop a tumor growth inhibition model for adult diffuse low-grade gliomas (LGG) able to describe tumor size evolution in patients treated with chemotherapy or radiotherapy.

Experimental Design: Using longitudinal mean tumor diameter (MTD) data from 21 patients treated with first-line procarbazine, 1-(2-chloroethyl)-3-cyclohexyl-l-nitrosourea, and vincristine (PCV) chemotherapy, we formulated a model consisting of a system of differential equations, incorporating tumor-specific and treatment-related parameters that reflect the response of proliferative and quiescent tumor tissue to treatment. The model was then applied to the analysis of longitudinal tumor size data in 24 patients treated with first-line temozolomide (TMZ) chemotherapy and in 25 patients treated with first-line radiotherapy.

Results: The model successfully described the MTD dynamics of LGG before, during, and after PCV chemotherapy. Using the same model structure, we were also able to successfully describe the MTD dynamics in LGG patients treated with TMZ chemotherapy or radiotherapy. Tumor-specific parameters were found to be consistent across the three treatment modalities. The model is robust to sensitivity analysis, and preliminary results suggest that it can predict treatment response on the basis of pretreatment tumor size data.

Conclusions: Using MTD data, we propose a tumor growth inhibition model able to describe LGG tumor size evolution in patients treated with chemotherapy or radiotherapy. In the future, this model might be used to predict treatment efficacy in LGG patients and could constitute a rational tool to conceive more effective chemotherapy schedules. *Clin Cancer Res; 18(18); 5071–80. ©2012 AACR.*

Introduction

The use of existing clinical data to model tumors' dynamic response to antitumor treatments is a promising approach toward improving treatment efficacy and accelerating the development of antitumor drugs. Such strategies have been applied, for example, to predict and monitor chemotherapy-induced myelosuppresion (1). In addition, tumor growth inhibition (TGI) models have successfully been developed to assess tumor size dynamics following cytotoxic treatment in non–small cell lung cancer (NSCLC; refs. 2, 3). In colorectal cancer, a TGI model was able to use data on tumor dynamics from a phase II study to predict overall survival in a subsequent phase III trial (4).

Herein we rely on clinical data to develop a TGI model for adult diffuse low-grade gliomas (LGG). LGGs are progressive brain tumors characterized radiologically by slow and continuous growth preceding anaplastic transformation (5, 6). Despite advancements in treatment methods in recent years, most LGGs remain incurable. LGG treatment approaches include surgery, radiotherapy, and chemotherapy with procarbazine, 1-(2-chloroethyl)-3-cyclohexyl-l-nitrosourea (CCNU), and vincristine (PCV) or temozolomide (TMZ; ref. 6).

Our model aims to capture the growth kinetics of LGG after chemotherapy or radiotherapy, and ultimately to serve as a rational tool that might provide insight into means of optimizing LGG treatment.

Authors' Affiliations: [1]INRIA, Project-team NUMED, Ecole Normale Supérieure de Lyon; [2]Hospices Civils de Lyon, Hôpital Neurologique, Neuro-oncologie; [3]EA3738 CTO, Faculté de Médecine Lyon-Sud, Oullins; Pharmacie, Hôpital de la Croix Rousse, Hospices civils de Lyon; [4]Université de Lyon, Claude Bernard Lyon 1; [5]Lyon Neuroscience Research Center INSERM U1028/CNRS UMR 5292, Lyon, France; [6]AP-HP, Groupe Hospitalier Pitié-Salpêtrière, Service de Neurologie Mazarin; INSERM, U975, Centre de Recherche de l'Institut du Cerveau et de la Moelle; Université Pierre & Marie Curie Paris VI, Faculté de médecine Pitié-Salpêtrière, CNRS UMR 7225 and UMR-S975; [7]Hôpital d'Instruction des Armées du Val-de-Grâce; [8]Service de Neuropathologie, Hôpital de la Salpêtrière; and [9]Service de Neurochirurgie, Centre Hospitalier Sainte-Anne, University Paris Descartes, Paris, France

Note: Supplementary data for this article are available at Clinical Cancer Research Online (http://clincancerres.aacrjournals.org/).

Corresponding Author: Benjamin Ribba, INRIA, Project-team NUMED, Ecole Normale Supérieure de Lyon, 46 allée d'Italie, 69007 Lyon Cedex 07, France. Phone:+334-766-152-00; Fax: +334-766-152-52; E-mail: benjamin.ribba@inria.fr

doi: 10.1158/1078-0432.CCR-12-0084

Published OnlineFirst July 3, 2012; DOI: 10.1158/1078-0432.CCR-12-0084

Translational Relevance

In this work, we propose a model of tumor growth inhibition that successfully describes the time course of tumor size [measured as mean tumor diameter (MTD)] in patients with low-grade glioma (LGG). We analyze MTD dynamics in patients treated with 3 different forms of first-line therapy—chemotherapy (temozolomide or procarbazine, 1-(2-chloroethyl)-3-cyclohexyl-l-nitrosourea, and vincristine) or radiotherapy—and show that model performance and parameter estimates are consistent across treatment modalities. This model might constitute a rational tool to predict treatment efficacy and to optimize treatment schedules in LGG patients.

In a previous study, we showed that after termination of PCV chemotherapy, LGGs frequently continue to decrease in volume despite chemotherapy no longer being administered (7, 8). One potential cause for this effect is delayed action of chemotherapy on quiescent tumor cells. This hypothesis is consistent with the cell-cycle nonspecific mechanism of action of the alkylating agents (procarbazine and especially CCNU) used in the PCV regimen (9). On the basis of this hypothesis, herein we use longitudinal tumor size data from patients treated with first-line PCV chemotherapy to formulate a TGI model in which LGGs consist of proliferative and quiescent tumor tissues that respond differently to treatment. We successfully use the model to analyze tumor size dynamics not only in patients treated with PCV chemotherapy but also in patients treated with TMZ chemotherapy or radiotherapy, and we show that the nontreatment-related parameters of the model are consistent across the 3 therapeutic modalities.

Material and Methods

Patients and data collection

We analyzed longitudinal tumor size measurements from LGG patients treated with first-line PCV chemotherapy ($n = 21$ patients), first-line TMZ chemotherapy ($n = 24$), or first-line radiotherapy ($n = 25$). These treatment methods represent the main LGG treatment modalities used in various institutions (PCV is used in Lyon; ref. 8; radiotherapy was used at the Salpêtrière Hospital in Paris until the 1990s and was subsequently replaced by TMZ; ref. 7). We did not consider surgery as a first-line treatment.

Patients left the study upon anaplastic transformation (histologically proven or suspected when rapidly growing foci of enhanced contrast appeared on imaging) or when tumor progression led to a need for a different form of treatment. Treatment was given either just after LGG diagnosis or after a follow-up period lasting up to several years.

The measurements analyzed in the 3 studies are shown in Fig. 1. Tumor size measurements were expressed as mean tumor diameters (MTD) in millimeter and were estimated manually from printed MRI images in which maximal radiological abnormalities were visible (5):

$\mathrm{MTD} = (2V)^{\frac{1}{2}}$, where $V = \frac{D_1 \times D_2 \times D_3}{2}$ is the approximated tumor volume with D_1, D_2, and D_3 referring to the 3 largest measured perpendicular diameters.

As shown in Fig. 1, the typical MTD curve is characterized by 4 phases: a slow-growing phase before treatment onset, a decrease in MTD upon treatment initiation, a prolongation (from months to several years) of this decrease after treatment termination, and a late and final regrowth phase.

PCV chemotherapy. We used tumor size data from a previously published study of a series of 21 LGG patients treated with first-line PCV, representing a total of 254 measurements (median, 12 points per patient; min., 4; max., 22; ref. 8). These patients (13 females and 8 males) had been treated at the Pierre Wertheimer Neurological Hospital and the Léon Bérard Cancer Center in Lyon between 1994 and 2005 (8). The baseline MTD (MTD at treatment) was 69 mm on average (median, 62 mm; min., 41 mm; max., 87 mm). The PCV protocol consisted of up to 6 cycles of the following treatment, with intervals of 6 weeks between cycles: CCNU (110 mg/m^2) administered on day 1, procarbazine (60 mg/m^2) administered on days 8 to 21, and vincristine (1.4 mg/m^2, max. 2 mg) administered on days 8 and 29. Median age at PCV onset was 47 years. Median duration of the observation period was 81 months. Medians of 3 observations before treatment and 12 observations after treatment were available for each patient. The histologic subtypes were grade II oligodendroglioma ($n = 15$), grade II oligoastrocytoma ($n = 4$), and grade II astrocytoma ($n = 2$).

TMZ chemotherapy. Tumor size data from 24 patients treated with first-line TMZ chemotherapy were used, representing a total of 294 measurements (median, 11 measurements per patient; min., 5; max., 23). These patients (14 females and 10 males) had been treated at the Salpêtrière Hospital between 2000 and 2005 (7). The baseline MTD was 51 mm on average (median, 48 mm; min., 26 mm; max., 85 mm). Treatment consisted of up to 30 cycles of TMZ administration; in each cycle, TMZ was administered orally from days 1 through 5 at a dose of 150 to 200 mg/m^2/d; administration was repeated every 28 days. Median age at TMZ onset was 45 years. Median duration of the observation period was 42 months. The median numbers of observations per patient were 3 and 8 before and after treatment onset, respectively. We used data for a limited number of patients ($n = 24$), randomly selected from a group of 120 patients for whom data were available (7). This allowed us to preserve homogeneity across the 3 treatment groups in terms of the number of subjects. However, the remaining 96 patients were used for external validation of the model. The histologic subtypes were grade II oligodendroglioma ($n = 20$), grade II oligoastrocytoma ($n = 3$), and grade II astrocytoma ($n = 1$).

Radiotherapy. We measured the time course of the MTD of 25 patients treated with first-line radiotherapy; measurements were carried out specifically for this study. We obtained a total of 249 measurements (median, 9

Published OnlineFirst July 3, 2012; DOI: 10.1158/1078-0432.CCR-12-0084

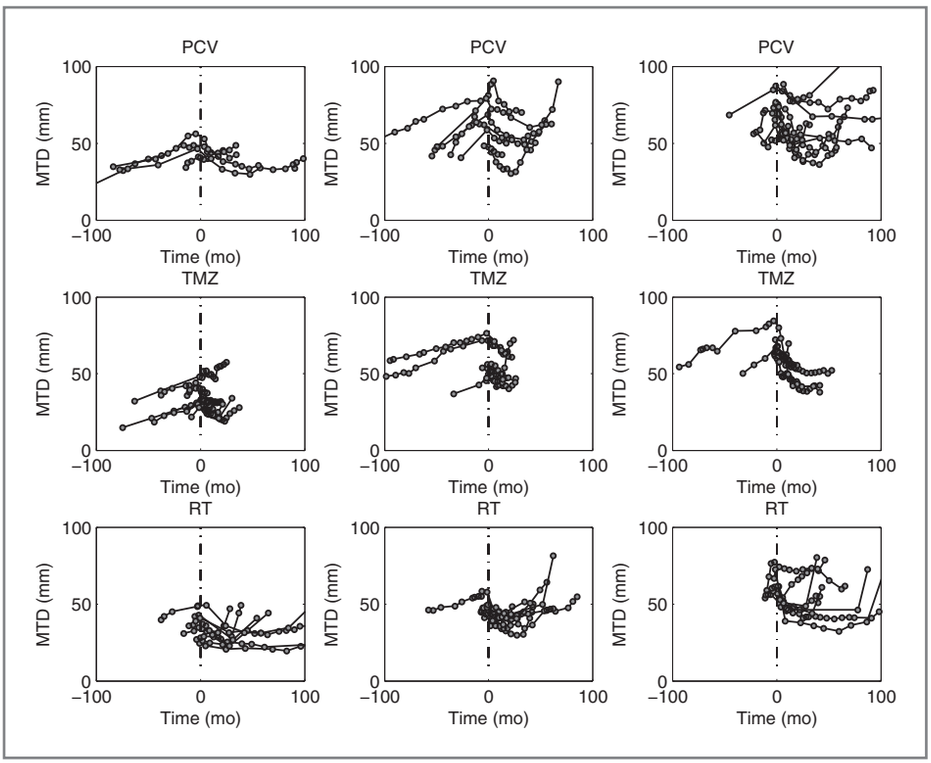

Figure 1. Mean tumor diameter (MTD) observations in patients treated with PCV chemotherapy (top), TMZ chemotherapy (middle), and radiotherapy (RT; bottom) as a function of time in months. Each column shows the trajectories of multiple patients who had similar MTDs at diagnosis. Time 0 corresponds to the time of treatment onset. In 19 patients treated with PCV (90%), 21 patients treated with radiotherapy (84%), and 21 patients treated with TMZ (87%), treatment was started only after a follow-up period lasting up to several years.

measurements per patient; min., 5; max., 21). These patients (11 females and 14 males) had been treated at the Salpêtrière Hospital between 1990 and 2001. Baseline MTD was 49 mm on average (median, 48 mm; min., 24 mm; max., 82 mm). Radiotherapy was administered daily at a median total dose of 54 Gy (min., 30 Gy; max., 60 Gy), with a median dose per fraction of 1.8 Gy. Median age at radiotherapy onset was 39 years. Median duration of the observation period was 65 months. Medians of 1 and 8 observations per patient were available before and after treatment, respectively. The histologic subtypes were grade II oligodendroglioma ($n = 7$), grade II oligoastrocytoma ($n = 6$), and grade II astrocytoma ($n = 12$).

Modeling technique

The tumor model we formulated belongs to the category of mixed-effects models (10). In this modeling technique, all individual data are analyzed simultaneously in order to provide information about the progression of each individual tumor. The modeling process comprises two steps. In the first step, a likelihood function is minimized to estimate the mean values of the model parameters as well as their interindividual variability throughout the population. The resulting estimates are called "population parameters." In the second step, we use information on the population parameters to estimate the best model parameters for each individual on the basis of his or her individual dataset. These parameters are called "individual parameters." The Monolix software (Lixoft), on the basis of the stochastic approximation of the expectation–maximization algorithm, was used to estimate the population and individual parameters (11). We evaluated the model according to goodness of fit, residual plots, and precision of parameter estimates as relative SEs. We calculated the ε-shrinkage and η-shrinkage to analyze the degree of shrinkage of individual predictions toward the observations (12). η-Shrinkage refers to shrinkage of the individual model parameters, and ε-shrinkage refers to residual error model parameters. In cases of low ε-shrinkage (<15%), individual predictions were considered to be reliable for model diagnostics. We also examined the normalized prediction distribution errors because this criterion is a powerful tool for detecting bias in model formulation with respect to available data (13). The prediction discrepancy of an observation is the percentile of that observation in the posterior distribution of the predicted MTD values, obtained by Monte Carlo simulations of the population model. By construction, the normalized prediction distribution errors follow a normal distribution with mean 0 and variance equal to 1.

Modeling strategy

To develop the model, we used longitudinal tumor size data from the 21 patients treated with PCV chemotherapy (Fig. 1). To select the best model from among multiple model structures, we used the objective function (OBJ $= -2 \times$ LLH), where LLH is the log likelihood value, and the Bayesian information criterion [BIC $= -2 \times$ LLH $+ \log(n)$ k], where k is the total number of parameters and n is the number of subjects. Additional information on the strategy used for model selection and evaluation is presented in the

Published OnlineFirst July 3, 2012; DOI: 10.1158/1078-0432.CCR-12-0084

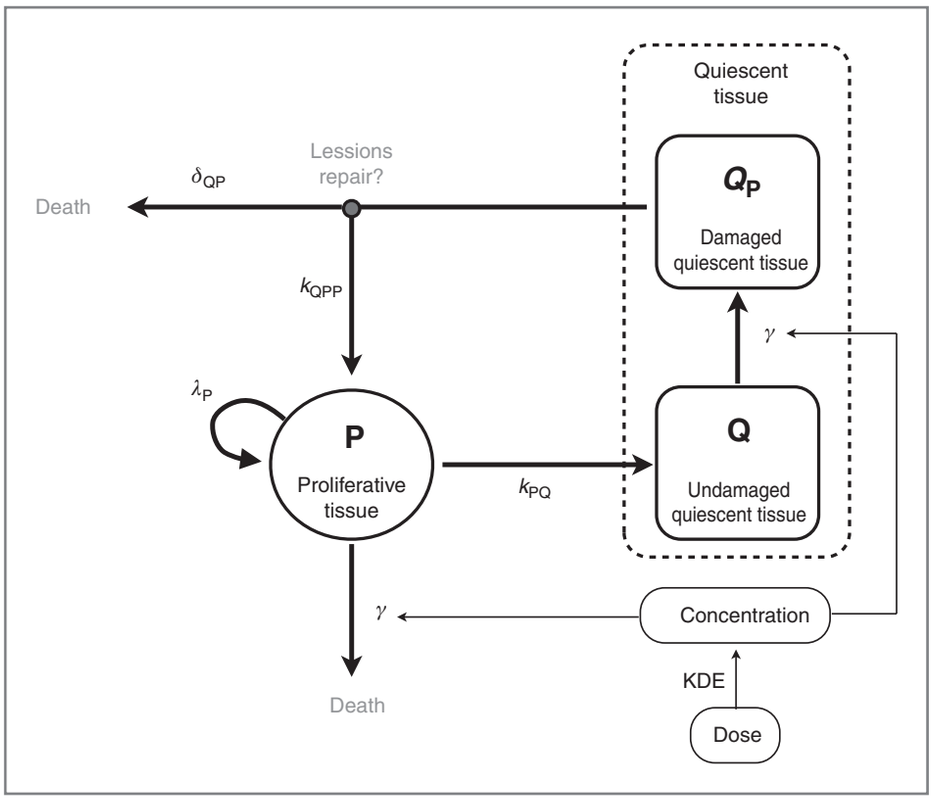

Figure 2. Schematic view of the model. *P* denotes the proliferative tissue and *Q* the nonproliferative or quiescent tissue. Proliferative tissue is assumed to transition to quiescence at a rate constant k_{PQ}. The treatment concentration, calculated from the individual dose through an exponential decay with the rate constant KDE, affects both proliferative and quiescent tissue. The tissue composed of cells in proliferation (*P*) is directly eliminated because of lethal DNA damages induced by the treatment. Nonproliferative tissue (*Q*) is also subject to DNA damages due to the treatment. When re-entering the cell cycle, the DNA-damaged quiescent cells (Q_P) can either repair their DNA damages and return to a proliferative state (*P*) or die because of unrepaired damages.

Supplementary data ("Model selection" section and Supplementary Fig. S1).

We chose to base the model development on the PCV dataset for 2 reasons. First, it seemed to us essential for our model to be able to describe the ongoing MTD decrease that occurs after treatment termination, hypothesized to be the result of the different responses to treatment of proliferative and quiescent cells. Posttreatment decreases in MTD were particularly obvious in patients treated with PCV chemotherapy (8). Second, the PCV dataset was the most complete, with the longest observation period and the most observations per patient before and after treatment.

Model development

The final selected model is shown in Fig. 2 and relies on the following structure. The tumor is composed of proliferative (P) and nonproliferative quiescent tissue (Q), expressed in millimeters. The transition of proliferative tissue into quiescence is governed by a rate constant denoted k_{PQ}. The treatment directly eliminates proliferative cells by inducing lethal DNA damage while cells progress through the cell cycle. The quiescent cells are also affected by the treatment and become damaged quiescent cells (Q_P). Damaged quiescent cells, when re-entering the cell cycle, can repair their DNA and become proliferative once again (transition from Q_P to *P*) or can die because of unrepaired damages (14, 15). This hypothesis is consistent with the mechanism of action of CCNU and procarbazine, which are alkylating agents considered to be cell-cycle nonspecific drugs that induce DNA damages in both proliferative and quiescent cells (9).

We modeled the pharmacokinetics of the PCV chemotherapy using a kinetic–pharmacodynamic approach, in which drug concentration is assumed to decay according to an exponential function (16). In this model, we did not consider the 3 drugs separately. Rather, we assumed the treatment to be represented as a whole by a unique variable (*C*), which represents the concentration of a virtual drug encompassing the 3 chemotherapeutic components of the PCV regimen. We modeled the exact number of treatment cycles administered by setting the value of *C* to 1 (arbitrary unit) at the initiation of each cycle (T_{Treat}): $C\,(t = T_{treat}) = 1$.

The resulting model is as follows:

$$\frac{dC}{dt} = -\mathrm{KDE} \times C$$

$$\frac{dP}{dt} = \lambda_p \times P\left(1 - \frac{P^*}{K}\right) + k_{Q_PP} \times Q_P - k_{PQ} \times P - \gamma_P \times C \times \mathrm{KDE} \times P$$

$$\frac{dQ}{dt} = k_{PQ}P - \gamma_Q \times C \times \mathrm{KDE} \times Q$$

$$\frac{dQ_P}{dt} = \gamma_Q \times C \times \mathrm{KDE} \times Q - k_{Q_PP}Q_P - \delta_{QP} \times Q_P$$

$$P^* = P + Q + Q_P$$

Published OnlineFirst July 3, 2012; DOI: 10.1158/1078-0432.CCR-12-0084

The parameter KDE is the rate constant for the decay of the PCV concentration in plasma, denoted C. λ_p is the rate constant of growth used in the logistic expression for the expansion of proliferative tissue (see below). The drug concentration (C) is assumed to induce DNA damages in both proliferative and quiescent tissue through linear functions (damages in proliferative and quiescent tissue are denoted γ_P and γ_Q, respectively). We assumed $\gamma_P = \gamma_Q = \gamma$ for identifiability reasons. However, this hypothesis can be justified by the fact that the basic action of the treatment may not depend on the cell-cycle status (proliferative or quiescent; ref. 9).

We tested different expressions (linear, exponential, logistic, generalized logistic, and Gompertz) for the growth of the proliferative tissue. A logistic term with a fixed maximal tumor size (K) of 100 mm provided the best results in terms of the objective function, and 100 mm is consistent with the maximal MTD usually observed in LGG patients (7). The parameter k_{QpP} denotes the rate constant for transfer from damaged quiescent tissue to proliferative tissue, and δ_{Qp} denotes the rate constant for elimination of the damaged quiescent tissue.

The model parameters were estimated by fitting the model solution $P + Q + Q_P$ to the actual MTD values. The resulting set of parameters to be estimated was $(\lambda_P, k_{PQ}, k_{QpP}, \delta_{Qp}, \gamma, \mathrm{KDE})$ with 2 additional initial conditions, $P_0 = P(t = 0)$ and $Q_0 = Q(t = 0)$, where time $(t = 0)$ corresponds to the first available data. We assumed $Q_{P_0} = Q_P(t = 0) = 0$in the absence of treatment.

The individual parameters corresponding to the 8 population parameters (6 parameters + 2 initial conditions) were assumed to be log normally distributed across individuals. For example, for the efficacy parameter γ, we set $\gamma_i = \gamma \times \exp(\eta_i)$, where γ is the mean (population) value, γ_i is the individual parameter value, and η_i represents the deviation for the individual i from the mean value. η are random variables with mean 0 and variance ω, estimated as part of the population parameters and expressed as coefficient of variation in percent. The variability on KDE was fixed. All remaining parameters were estimated with their interindividual variability. We assumed potential correlations between the random effects. Patient characteristics such as sex, tumor type (oligodendroglioma, oligoastrocytoma, or astrocytoma), age at diagnosis, and age at treatment onset were tested as potential covariates of model parameters.

In this model, λ_P(the rate constant of growth for the proliferative tissue) and k_{PQ} (the rate constant for transition from proliferation to quiescence) are considered to be tumor-specific parameters, as in the absence of treatment, the model system shrinks to a system in which only these 2 parameters regulate tumor growth. The remaining parameters $(k_{QpP}, \delta_{Qp}, \gamma, \mathrm{KDE})$ can be considered as treatment-related parameters. Note, however, that all parameters regulate together the characteristics of tumor response to treatment, especially tumor shrinkage and duration of response.

TMZ chemotherapy and radiotherapy. Using the model structure developed for the analysis of the PCV data, we analyzed separately the data from patients treated with TMZ chemotherapy and the data from patients treated with radiotherapy. TMZ (like CCNU and procarbazine) is an alkylating agent and thus is considered to be cell-cycle nonspecific. Radiotherapy is also known to be cell-cycle nonspecific and to induce DNA damages in both proliferative and quiescent cells (9). Therefore, it seemed to us justified to model these two treatments using the model structure developed for PCV chemotherapy. For TMZ chemotherapy, however, because the treatment scheduling was much more variable between patients, we did not take into account the number of cycles administered to the patients. We only considered a single treatment cycle and set the virtual TMZ concentration to 1 at the time of treatment initiation. MTD in patients treated with radiotherapy was ultimately modeled in the same way. We did initially attempt to model the effect of radiation differently by relying on an on/off switching hypothesis. Specifically, we initially assumed that during the treatment period, the tissue was affected through the parameter γ, and outside the treatment period this effect was removed, that is, γ was set to 0. However, we later adopted the use of the kinetic–pharmacodynamic approach, as it did not affect the objective function and enabled us to compare parameter values across treatments.

Results

Model parameter estimates and model evaluation

The selected structural model (Fig. 2) successfully described the tumor size dynamics before, during, and after treatment in patients treated with first-line PCV chemotherapy and also in patients treated with first-line TMZ chemotherapy or first-line radiotherapy. Figure 3 shows predicted MTD values plotted against observed MTD values for all patients in each of the 3 groups and reveals a strong correlation between predictions and observations, showing that the model correctly reproduced, without any apparent bias, the observed MTD values. Figure 4 depicts the observed MTD values together with the model predictions, using the individual parameters of 3 representative patients from each treatment series. Again, a strong correlation was evident between the observed and the predicted evolution patterns of the MTD in these patients.

We carried out sensitivity analysis for the model in the 21 patients treated with PCV. This analysis consisted of repeating the estimations while leaving out 1 patient's data in each repetition. It appears that no single patient substantially influenced the estimation (results shown in the Supplementary data: "Sensitivity of parameter estimates" and Supplementary Fig. S2).

We also investigated the effect of the choice of the variability level of parameter KDE, the rate constant for the decay of the PCV concentration in plasma. We initially attempted to estimate the variability on *KDE*, but its estimation was found to be associated with a high SE and a worsening of the objective function. For these reasons,

Published OnlineFirst July 3, 2012; DOI: 10.1158/1078-0432.CCR-12-0084

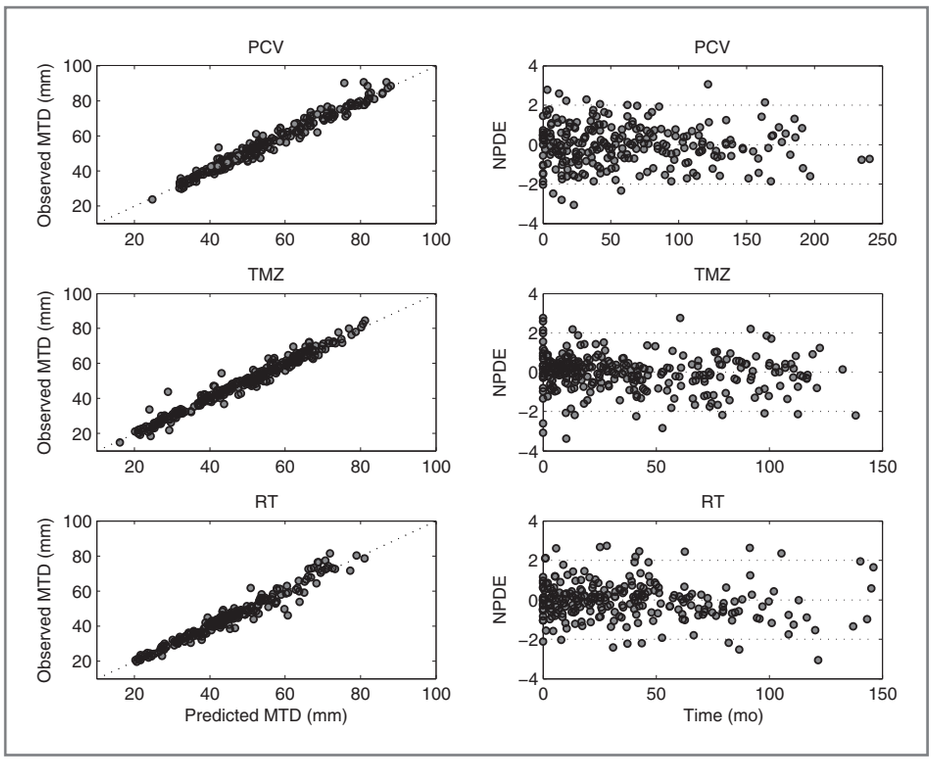

Figure 3. Observations versus individual predictions including lines of identity (left) and normalized prediction distribution errors (NPDE) versus time (right) for PCV chemotherapy (top), TMZ chemotherapy (middle), and radiotherapy (RT; bottom). As expected, the NPDE distribution is similar to a normal distribution with mean 0 and variance equal to 1. The ε-shrinkage was 9% for PCV predictions, 7% for TMZ, and 14% for radiotherapy.

we assigned a fixed value to the variability. In the model, we set this variability level at a high percentage, 70%, in order to accommodate the simplistic approach used to model treatment pharmacokinetics. However, further analysis shows that parameter estimates are not significantly affected when this variability is set to 0 (Supplementary data: "Sensitivity of parameter estimates" and Supplementary Fig. S3).

We also used the stepwise-backward strategy (17) to investigate whether any patient characteristics functioned as model covariates; none of the examined characteristics was identified as a covariate.

As shown in Table 1, consistent with the model's assumption that λ_P and k_{PQ} are tumor specific, the independent estimation of these 2 parameters resulted in consistent values across the 3 data series. The basic doubling times of the size of the proliferative tissue, expressed as the inverse of the growth parameter ($1/\lambda_P$), were estimated to be 8.3, 8.8, and 7.3 months for the PCV, TMZ, and radiotherapy data series, respectively. The growth rate of the proliferative tissue was estimated to be 4 to 5.5 times higher than its quiescence rate.

For patients treated with radiotherapy, we initially estimated that the rate of transition of damaged quiescent tissue into a proliferative state (k_{Q_DP}) was very low ($<10^{-5}$). This seems to indicate that quiescent cells that have sustained DNA damages from radiotherapy are likely to die when re-entering the cell cycle. This estimation, however, was associated with a substantial relative SE (>100%). For PCV and TMZ chemotherapy, we estimated that 20% to 25% of damaged quiescent cells could repair their lesions to reconstitute the pool of proliferative cells.

External validation and potential for prediction

To investigate the validity of the model, we used the data from the remaining 96 patients treated with TMZ who were not included in the sample for parameter estimation. We compared the MTD time course observed in this series with the MTD time course simulated with the model using the parameter estimates of the original sample of 24 patients treated with TMZ. The results of this analysis, presented in Fig. 5 (left), show good agreement between the 5%, 50%, and 95% observed percentiles and the 5%, 50%, and 95% simulated percentiles of the MTD time course.

We then explored the model's ability to predict treatment efficacy in LGG patients on the basis of pretreatment time-course tumor size observations. To this end, we pooled together the PCV and radiotherapy data to constitute a database of 46 patients. Six LGGs treated with PCV chemotherapy were randomly selected out of the database. We used the remaining 40 patients to estimate population parameters by introducing the type of treatment (PCV chemotherapy or radiotherapy) as a covariate on the efficacy parameter γ by following the stepwise-backward method (17). Parameter estimates in the pooled dataset were similar to those obtained in previous estimations (see Supplementary data: "Sensitivity of parameter estimates" and Supplementary Fig. S4). For the 6 patients whose data we isolated from the group, we predicted the MTD time course by using the population parameter estimates, except for the tumor-specific λ_P parameter, which we estimated for each patient

Published OnlineFirst July 3, 2012; DOI: 10.1158/1078-0432.CCR-12-0084

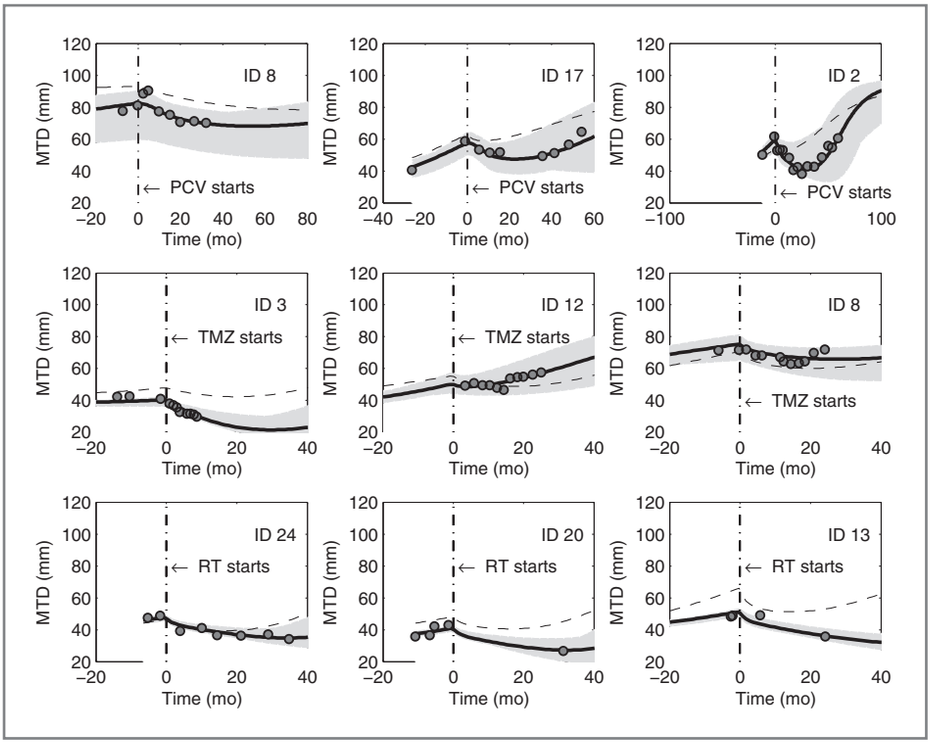

Figure 4. MTD observed (circles), individual predictions (solid line), and population predictions on the basis of mean parameter values (dashed line) for 3 individuals in each study (top, PCV; middle: TMZ; bottom, RT) selected on the basis of their typical residual error magnitude (the individual's average absolute weight residual is at the population median). Included is the 90% confidence interval around the individual predictions obtained by simulation using the SEs of the empirical Bayes estimates.

according to his or her individual pretreatment MTD data. At least 2 pretreatment data points are required to estimate this growth parameter. The initial conditions P_0 and Q_0 were assigned using the actual MTD observation at diagnosis (corresponding to $P_0 + Q_0$) and assuming that the proliferative tissue constitutes 10% of the whole tumor size (18). As shown in Fig. 5 (right), there was good correlation between the predicted and the observed MTD time courses in these 6 patients ($r^2 = 0.86$, $P < 0.001$ for the 6 patients, representing 52 predictions). This suggests that the model might be used to predict treatment efficacy on the basis of population parameter estimates combined with individual estimations of the tumor growth rate parameter. The 6 individual prediction profiles are presented in the Supplementary data (Supplementary Fig. S5).

Discussion

We have developed a TGI model that successfully reproduces tumor size dynamics of LGG patients treated with chemotherapy (PCV or TMZ) or radiotherapy. The slow growth of LGGs and the ongoing response that is frequently observed after treatment termination led us to formulate a model that was more complex than the existing TGI models for NSCLC and colorectal cancer, which use linear (2) or exponential functions (4) to model tumor growth. Those simple models would be insufficient to reproduce our data, and specifically, they would be unable to capture the prolonged response of the tumor following cessation of treatment. We provide a biological interpretation for this prolonged response, attributing it to delayed treatment action on quiescent cells as compared with proliferative cells, and represent it in our model by incorporating both proliferative (P) and quiescent cell populations. These populations respond differently to the therapeutic modalities typically used in the treatment of LGG, which all function by damaging the DNA of both cells in both populations (9).

The model is composed of 4 ordinary differential equations and incorporates 6 parameters and 2 initial conditions. Two parameters (λ_P and k_{PQ}) are considered to be tumor-specific parameters, as in the absence of treatment the complexity of the model shrinks to a system regulated by these 2 parameters alone. The remaining 4 parameters are considered to be treatment-related parameters.

Importantly, independent analyses of patients treated with PCV chemotherapy, TMZ chemotherapy, or radiotherapy produced similar estimates of tumor-specific parameters (λ_P and k_{PQ}). Estimated parameters were also consistent with known biological characteristics of LGG. For example, according to the model, LGGs mostly consist of quiescent cells. Estimates indicated that the initial proliferative tissue represented 2% of the tumor in the TMZ series, 9% in the radiotherapy series, and 15% in the PCV chemotherapy series (see Table 1). In LGG, the proliferative tissue, as measured by Ki-67 labeling, is typically less than 5%; however, Ki-67 labeling indices of up to 10% have been observed (18). Furthermore, the Ki-67 labeling index might underrepresent the quantity of proliferative tissue (19), and studies using MCM2 labeling have shown that approximately 9% of the LGG may be proliferative tissue (20). Indeed, MCM2 stains not only cycling cells but also cells that are licensed for DNA replication. Biologic validation of the model will require an investigation of the correlation

Published OnlineFirst July 3, 2012; DOI: 10.1158/1078-0432.CCR-12-0084

Table 1. Model parameter estimates for patients in the 3 studies

		PCV		TMZ		Radiotherapy	
Parameters	**Unit**	**Mean value**	**CV (%)**	**Mean value**	**CV (%)**	**Mean value**	**CV (%)**
P_0	mm	7.13 (25)	94 (23)	0.924 (57)	112 (22)	3.89 (28)	67 (68)
Q_0	mm	41.2 (7)	54 (10)	42.3 (8)	62 (12)	40.3 (6)	49 (12)
λ_P	mo^{-1}	0.121 (16)	72 (9)	0.114 (29)	66 (19)	0.138 (16)	62 (18)
k_{PQ}	mo^{-1}	0.0295 (21)	76 (12)	0.0226 (54)	87 (21)	0.0249 (41)	89 (28)
k_{Q_PP}	mo^{-1}	0.0031 (35)	97 (31)	0.0045 (70)	113 (9)	—	—
δ_{QP}	mo^{-1}	0.00867 (21)	75 (12)	0.0214 (34)	76 (34)	0.0125 (29)	97 (18)
γ	—	0.729 (37)	115 (9)	0.842 (43)	107 (13)	1.71 (24)	83 (20)
KDE	mo^{-1}	0.24 (33)	70 (fixed)	0.32 (34)	70 (fixed)	0.317 (60)	70 (fixed)

Parameters are defined in the text. Interindividual variability (CV) is expressed as percentages. The errors on the estimates are shown in parentheses and were computed as the ratio between the SE and the parameter estimate multiplied by 100. The 95% confidence intervals can then be calculated as follows: value $\pm$ 1.96 $\times$ SE. The values for tumor-specific parameters (λ_P and k_{PQ}) were found to be very similar across treatments. For the patients treated with PCV chemotherapy, the median η-shrinkage was 6% and the maximum value was 29% for parameter k_{Q_PP}. For TMZ chemotherapy, the median η-shrinkage was 14%. Parameters k_{PQ} and δ_{QP} were associated with the highest η-shrinkage (32% and 25%, respectively). For radiotherapy, the median η-shrinkage was 7%. Parameters *KDE* and k_{PQ} were associated with the highest η-shrinkage (36% and 23%, respectively).

between λ_P (the growth rate of the proliferative tissue) and quantities of proliferative tissue observed through Ki-67 labeling. It will also be important to assess whether taking into account molecular characteristics of LGG, namely, the 1p/19q codeletion status, the IDH1 mutation status, and the MGMT methylation status (21), might improve the model's accuracy.

A particularly interesting aspect of our model lies in its ability to simulate the time course of the quantity of proliferative tissue in treated LGG. As the proliferation index in LGG has been correlated with the ratio of choline/*N*-acetylaspartate (NAA), measured using MRI spectroscopy (22), assessment of the choline/NAA ratio time course in treated LGG could be used to validate our model's predictions regarding the growth patterns of proliferative tissue. The validated model could then be used as a simulation tool to conceive potentially more effective treatment schedules. For example, model simulations with different durations of chemotherapy or different time intervals between chemotherapy cycles could assist in identifying chemotherapy schedules with a more prolonged impact on proliferative cells.

Another promising avenue would be to use the model to predict treatment efficacy in LGG patients on the basis of pretreatment time-course tumor size observations. Simulations of response to different treatments (chemotherapy or radiotherapy, for example) or to different chemotherapy regimens (PCV or TMZ, for example) could be conducted to

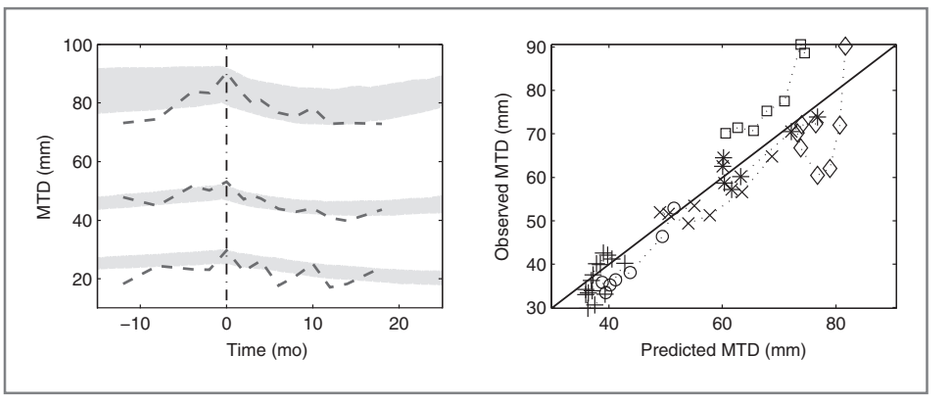

Figure 5. Left, observed 5%, 50%, and 95% percentiles on 96 external patients treated with TMZ (dashed line) with the corresponding simulated percentiles using parameters estimated for the initial set of 24 TMZ-treated patients. The simulated percentiles were calculated on the basis of 200 simulations of the model with 200 virtual individuals. Note that the low number of individual measurements after month 22 precludes comparison beyond that time. Right, predicted versus observed MTD data in 6 LGG patients treated with PCV chemotherapy. Different plotting characters are used to distinguish among the 6 patients. MTD values were predicted using pretreatment MTD data only ($r^2 = 0.86$, $P < 0.001$ for the 6 patients, representing 52 measurements). Pretreatment MTD data were used to estimate the tumor-specific λ_P parameter in each patient. The other parameters were estimated using the population parameters of 40 LGG patients treated with PCV chemotherapy ($n = 15$) or radiotherapy ($n = 25$).

Published OnlineFirst July 3, 2012; DOI: 10.1158/1078-0432.CCR-12-0084

select the most effective treatment for a given patient. As shown in the present study, preliminary data suggest that such an approach might be feasible, and future studies will have to investigate this potential on a larger number of patients.

Finally, we note that previous studies have made significant contributions toward modeling the time and space evolution of gliomas. These models, on the basis of partial differential equations (PDE), describe the spatiotemporal evolution patterns of tumor cells in the brain as "traveling waves" driven by 2 processes: uncontrolled proliferation and tissue invasion (23). This proliferation-invasion description has led to the suggestion that tumor diameter grows linearly over time with a velocity given by a combination of the 2 model parameters (24). Swanson and colleagues showed the relevance of such a model for the prediction of the growth kinetics of untreated gliomas, specifically estimating net rates of proliferation and invasion *in vivo* for individual patients (25, 26). These parameters were shown to be prognostic of overall survival and predictive of radiotherapy efficacy in glioblastoma (27, 28). Mandonnet and colleagues studied the reliability of this model in determining LGG dynamics (5, 29) and showed it to be in agreement with the linear evolution of the MTD observed in these tumors before transformation toward a higher grade of malignancy. As mixed-effect modeling techniques cannot be yet applied to PDEs, we were constrained to modeling the dynamic evolution of the MTD using ordinary differential equations, thus omitting any spatial considerations. In the future, the integration of nonlinear time and space models of tissue dynamics in a population context will certainly be the most efficient strategy to lead to an integrative, holistic model of LGG response to treatments (30).

In conclusion, we have developed a model of tumor growth inhibition that, to our knowledge, is the first to successfully describe the time course of tumor size in LGG patients treated with chemotherapy or radiotherapy. We believe that this model constitutes an important step toward developing rational strategies for predicting treatment efficacy and optimizing treatment schedules in LGG patients.

Disclosure of Potential Conflicts of Interest

F. Ducray had travel grants to attend ASCO by Roche. No potential conflicts of interest were disclosed by other authors.

Authors' Contributions

Conception and design: B. Ribba, G. Kaloshi, B. Čajavec-Bernard, J. Pallud, E. Grenier, F. Ducray
Development of methodology: B. Ribba, D. Richard, M. Tod, L. Dainese, E. Grenier, F. Ducray
Acquisition of data (provided animals, acquired and managed patients, provided facilities, etc.): G. Kaloshi, M. Peyre, S. Cartalat-Carel, J.-Y. Delattre, J. Honnorat, F. Ducray
Analysis and interpretation of data (e.g., statistical analysis, biostatistics, computational analysis): B. Ribba, M. Tod, L. Dainese, E. Grenier, F. Ducray
Writing, review, and/or revision of the manuscript: B. Ribba, G. Kaloshi, D. Richard, M. Tod, B. Čajavec-Bernard, A. Idbaih, D. Psimaras, J. Pallud, J.-Y. Delattre, J. Honnorat, F. Ducray
Administrative, technical, or material support (i.e., reporting or organizing data, constructing databases): B. Ribba, G. Kaloshi, J. Honnorat
Study supervision: B. Ribba, E. Grenier, F. Ducray

Acknowledgments

The authors wish to acknowledge Emmanuel Mandonnet and Samuel Bernard for valuable advice and discussions and Marie Aline Renard for her valuable help collecting data.

Grant Support

B. Čajavec-Bernard was funded by the ETOILE project consortium: "Espace de Traitement Oncologique par Ions Légers dans le cadre Européen."

The costs of publication of this article were defrayed in part by the payment of page charges. This article must therefore be hereby marked *advertisement* in accordance with 18 U.S.C. Section 1734 solely to indicate this fact.

Received January 10, 2012; revised June 18, 2012; accepted June 18, 2012; published OnlineFirst July 3, 2012.

References

1. Friberg LE, Henningsson A, Maas H, Nguyen L, Karlsson MO. Model of chemotherapy-induced myelosuppression with parameter consistency across drugs. J Clin Oncol 2002;20:4713–21.
2. Wang Y, Sung C, Dartois C, Ramchandani R, Booth BP, Rock E, et al. Elucidation of relationship between tumor size and survival in non–small-cell lung cancer patients can aid early decision making in clinical drug development. Clin Pharmacol Ther 2009;86:167–74.
3. Tham LS, Wang L, Soo RA, Lee SC, Lee HS, Yong WP, et al. A pharmacodynamic model for the time course of tumor shrinkage by gemcitabine + carboplatin in non–small cell lung cancer patients. Clin Cancer Res 2008;14:4213–8.
4. Claret L, Girard P, Hoff PM, Van Cutsem E, Zuideveld KP, Jorga K, et al. Model-based prediction of phase III overall survival in colorectal cancer on the basis of phase II tumor dynamics. J Clin Oncol 2009;27:4103–8.
5. Mandonnet E, Delattre JY, Tanguy ML, Swanson KR, Carpentier AF, Duffau H, et al. Continuous growth of mean tumor diameter in a subset of grade II gliomas. Ann Neurol 2003;53:524–8.
6. Soffietti R, Baumert BG, Bello L, von Deimling A, Duffau H, Frenay M, et al. Guidelines on management of low-grade gliomas: report of an EFNS-EANO* task force. Eur J Neurol 2010;17:1124–33.
7. Ricard D, Kaloshi G, Amiel-Benouaich A, Lejeune J, Marie Y, Mandonnet E, et al. Dynamic history of low-grade gliomas before and after temozolomide treatment. Ann Neurol 2007;61:484–90.
8. Peyre M, Cartalat-Carel S, Meyronet D, Ricard D, Jouvet A, Pallud J, et al. Prolonged response without prolonged chemotherapy: a lesson from PCV chemotherapy in low-grade gliomas. Neuro Oncol 2010;12:1078–82.
9. Chabner BA, Longo DL. Cancer chemotherapy and biotherapy: principles and practice. 3rd ed. Philadelphia, PA: Lippincott Williams & Wilkins; 2001.
10. Lindstrom ML, Bates DM. Nonlinear mixed effects models for repeated measures data. Biometrics 1990;46:673–87.
11. Samson A, Lavielle M, Mentre F. The SAEM algorithm for group comparison tests in longitudinal data analysis based on non-linear mixed-effects model. Stat Med 2007;26:4860–75.
12. Karlsson MO, Savic RM. Diagnosing model diagnostics. Clin Pharmacol Ther 2007;82:17–20.
13. Brendel K, Comets E, Laffont C, Laveille C, Mentre F. Metrics for external model evaluation with an application to the population pharmacokinetics of gliclazide. Pharm Res 2006;23:2036–49.
14. Kaina B. DNA damage-triggered apoptosis: critical role of DNA repair, double-strand breaks, cell proliferation and signaling. Biochem Pharmacol 2003;66:1547–54.

Published OnlineFirst July 3, 2012; DOI: 10.1158/1078-0432.CCR-12-0084

15. Masunaga S, Ono K, Hori H, Suzuki M, Kinashi Y, Takagaki M, et al. Potentially lethal damage repair by total and quiescent tumor cells following various DNA-damaging treatments. Radiat Med 1999;17:259–64.
16. Jacqmin P, Snoeck E, van Schaick EA, Gieschke R, Pillai P, Steimer JL, et al. Modelling response time profiles in the absence of drug concentrations: definition and performance evaluation of the K-PD model. J Pharmacokinet Pharmacodyn 2007;34:57–85.
17. Wahlby U, Jonsson EN, Karlsson MO. Comparison of stepwise covariate model building strategies in population pharmacokinetic–pharmacodynamic analysis. AAPS Pharm Sci 2002;4:E27.
18. Pallud J, Varlet P, Devaux B, Geha S, Badoual M, Deroulers C, et al. Diffuse low-grade oligodendrogliomas extend beyond MRI-defined abnormalities. Neurology 2010;74:1724–31.
19. Freeman A, Morris LS, Mills AD, Stoeber K, Laskey RA, Williams GH, et al. Minichromosome maintenance proteins as biological markers of dysplasia and malignancy. Clin Cancer Res 1999;5:2121–32.
20. Wharton SB, Chan KK, Anderson JR, Stoeber K, Williams GH. Replicative Mcm2 protein as a novel proliferation marker in oligodendrogliomas and its relationship to Ki67 labelling index, histological grade and prognosis. Neuropathol Appl Neurobiol 2001;27:305–13.
21. Kim YH, Nobusawa S, Mittelbronn M, Paulus W, Brokinkel B, Keyvani K, et al. Molecular classification of low-grade diffuse gliomas. Am J Pathol 2010;177:2708–14.
22. Tamiya T, Kinoshita K, Ono Y, Matsumoto K, Furuta T, Ohmoto T. Proton magnetic resonance spectroscopy reflects cellular proliferative activity in astrocytomas. Neuroradiology 2000;42:333–8.
23. Tracqui P, Cruywagen GC, Woodward DE, Bartoo GT, Murray JD, Alvord EC Jr. A mathematical model of glioma growth: the effect of chemotherapy on spatio-temporal growth. Cell Prolif 1995;28:17–31.
24. Murray JD. Mathematical biology. 3rd ed. New York: Springer; 2002.
25. Swanson KR, Alvord EC Jr, Murray JD. Virtual brain tumours (gliomas) enhance the reality of medical imaging and highlight inadequacies of current therapy. Br J Cancer 2002;86:14–8.
26. Swanson KR, Bridge C, Murray JD, Alvord EC Jr. Virtual and real brain tumors: using mathematical modeling to quantify glioma growth and invasion. J Neurol Sci 2003;216:1–10.
27. Harpold HL, Alvord EC Jr, Swanson KR. The evolution of mathematical modeling of glioma proliferation and invasion. J Neuropathol Exp Neurol 2007;66:1–9.
28. Wang CH, Rockhill JK, Mrugala M, Peacock DL, Lai A, Jusenius K, et al. Prognostic significance of growth kinetics in newly diagnosed glioblastomas revealed by combining serial imaging with a novel biomathematical model. Cancer Res 2009;69:9133–40.
29. Mandonnet E, Pallud J, Clatz O, Taillandier L, Konukoglu E, Duffau H, et al. Computational modeling of the WHO grade II glioma dynamics: principles and applications to management paradigm. Neurosurg Rev 2008;31:263–9.
30. Bonate PL. Pharmacokinetics in drug development: advances and applications. Vol. 3. New York, Heidelberg, Dordrecht, London: Springer; 2011.

Published OnlineFirst July 3, 2012; DOI: 10.1158/1078-0432.CCR-12-0084

Clinical Cancer Research

A Tumor Growth Inhibition Model for Low-Grade Glioma Treated with Chemotherapy or Radiotherapy

Benjamin Ribba, Gentian Kaloshi, Mathieu Peyre, et al.

Clin Cancer Res 2012;18:5071-5080. Published OnlineFirst July 3, 2012.